

**COB-2023-1536**

## **THERMO-HYDRAULIC EXPERIMENTAL ANALYSIS OF MULTI-MICROCHANNEL HEAT EXCHANGERS**

**Erick Daniel Rincón Castrillo**

**Frank Wiliam Adolfo Blanco Ojeda**

**Gleyzer Martins**

**Oscar Saul Hernandez Mendonza**

**Enio Pedone Bandarra Filho**

Federal University of Uberlândia

e-mails: daniel.rinconc@ufu.br; frank\_blanco@ufu.br; gmartins@ufu.br; oscarshm5@gmail.com; bandarra@ufu.br.

**Abstract.** *Microchannels are a heat dissipation technology that emerged for applications where there is a high concentration of energy, such as applications in microelectronic circuits and third-generation photovoltaic generation with solar concentration. Thus, the analysis of the thermo-hydraulic performance of multi-microchannel heat exchangers with rectangular geometry was developed. For the analysis, water was used as the working fluid with different values of mass flow, heating powers and inlet temperatures in the heat exchanger. The microchannel heat exchanger was experimentally tested with the imposed heat flux varying between 7.29 – 51.09 kW/m<sup>2</sup>, mass flow rate between 29 – 116 kg/s.m<sup>2</sup>, microchannel inlet temperature of 25 and 45°C. The heat transfer values for the base fluid in a fully developed laminar regime were compared with classical models for microchannel heat exchangers, with the Shah and London correlation showing the best agreement when compared with the experimental data. In hydraulic terms, the values of the friction factor are in accordance with the classical theory of fluid mechanics.*

**Keywords:** *Microchannel Heat Exchangers, Water, Thermo-Hydraulic Performance.*

### **1. INTRODUCTION**

The need to dissipate large amounts of heat in electronic devices to maintain life has led to the development of microchannel heat exchangers, introduced by Tuckerman and Pease (1981). These exchangers use a cooling fluid, which can be pure fluids, mixtures, or with nanofluids, as discussed by Rincón (2022).

The flow conditions influence the overall microchannel heat exchangers performance, in the literature there are works where laminar and turbulent flow conditions are used. Sharma et al. (2013) in their studies employed turbulent flow in the feed tubes (manifolds) and laminar flow in the microchannel heat sink. In the Mohammed Adham et al. (2013) review was observed that works with laminar flow conditions are the most common, which increases the performance of the exchangers, in addition, the channels dimensions prevent turbulence development.

Another aspect studied by Zhong et al. (2014) was the fluid application with phase change, they experimentally analyzed the heat transfer during condensation of a liquid-vapor separation microchannel condenser compared to the common parallel flow microchannel condenser, the results allowed establishing that the average heat transfer coefficient in condensation was higher than common parallel flow exchangers.

The microchannel heat exchangers improvement involves the proper heat flux distribution in the heat transfer core, as studied by Morini and Brandner (2018), the study of the geometry, as shown in the works on rectangular (Yang and Du, 2020; Kim, 2016), circular (Mukesh Kumar and Arun Kumar, 2020) and hexagonal (Alfaryjat et al., 2018) geometry and the study of heat sinks in the inlet and the outlet, as raised by Xia et al. (2015) and by Anbumeenakshi and Thansekhar (2014).

The demand for higher electronic circuit performances associated with microchannels has led to the study and development of differentiated geometries, as addressed by Lee et al. (2012), who made a comparison between microchannel exchangers with continuous fins and microchannel exchangers with 27° inclined sectional oblique fins, which allowed to establish oblique finned microchannel increased and uniform the heat transfer performance, relative to the conventional microchannel. Similarly, Xia et al. (2015) developed an experimental and numerical study of the influence of semicircular cavities along the channel walls on the microchannel performance compared to channels with the same dimensions but with rectangular geometry, with results showing a 1.24% reduction in thermal performance and an 18.99% reduction in pumping power. Khoshvaght-Aliabadi et al. (2017) also conducted an experimental and numerical study comparing rectangular microchannels with wavy microchannels by varying the microchannel waves frequency and concluded that the wavy along the microchannel walls increases heat transfer by causing chaotic advection in the working fluid. Another experimental and numerical study by researchers Khoshvaght-Aliabadi et al. (2017b) analyzed the flow

and heat transfer of straight and wavy miniature heat sinks (MHSs) with pin-fin interruptions, where the experimental results allowed them to establish that interrupted MHSs had better hydrothermal performance.

In the same way, micro ribbing in microchannels was experimentally analyzed by Esmaili et al. (2018) in which the results showed that the ribbed channel with 45° angle had the Nusselt number 3.5 times that of the flat channel and the use of ribbing in the microchannel showed up to 80% reduction in thermal resistance. Pan et al. (2019) conducted a comparative experimental study between conventional rectangular walled microchannels with rectangular walled microchannels with semicircular cavities along the wall, and the microchannel that showed the best heat transfer performance was with cavities spaced apart at the beginning and concentrated at the end. Peng et al. (2021) experimentally analyzed microchannels with zigzag channels to verify the influence of the incidence angle on microchannel performance, and the analysis of the experimental results showed that the smaller the incidence angle the better the hydraulic performance as a consequence of a lower pressure drop and friction between the fluid and the microchannel walls.

Finally, Pandey et al. (2022) performed a comparison between parallel microchannels and pin-fin heat sinks, concluding that the parallel microchannel heat sink showed better performance compared to the pin-fin heat sink and fins, however, the pressure drop was more favorable for the pin-fin fin heat sink.

In this work it was developed the experimental analysis of the thermal-hydraulic heat exchangers performance with rectangular microchannels, due to the simplicity of construction and water as a working fluid. Enabling the comparative analysis of the heat transfer coefficient in the channels with the classic convection correlations.

## 2. METHODOLOGY

### 2.1 Active cooling system

In the study of the active cooling system was used a rectangular section microchannel heat exchanger. This device used in this research, was designed, and mechanized by Fernandes (2017) being developed at the Laboratory of Nano, Microfluidics and Microsystems LabMEMS/COPPE/UFRJ.

Fernandes (2017) designed a micro heat exchanger proposing an optimized geometry for a heat exchanger with 24 microchannels with rectangular section of 400 μm wide, 945 μm high and 13 mm long and inlet/outlet plenum of trapezoidal shape. In order to increase the active cooling area and decrease the microchannel differences.

Figure 1 shows a microchannel heat exchanger exploded view. It has 6 standard M3 threaded holes, which comprise the effective cooling exchanger area. It consists of the fluid inlet/outlet plenum and the microchannels. It is important to point out that the holes located under the micro exchanger centerline help fixing this device to the surface to be cooled by means of nuts with a through bolt. The holes located at the corners are used to join the micro exchanger base and cover. The micro exchanger cover can also be seen, which has two standard M5 thread holes. The holes have the function of containing the two connection pieces of the quick coupling with M5 thread and the 4 mm hose inlet. Figure 2 illustrates the main geometric parameters used in the heat transfer calculation in the microchannel heat exchanger. Table 1 shows the values of the geometric parameters of the microchannel heat exchanger shown in Figure 2.

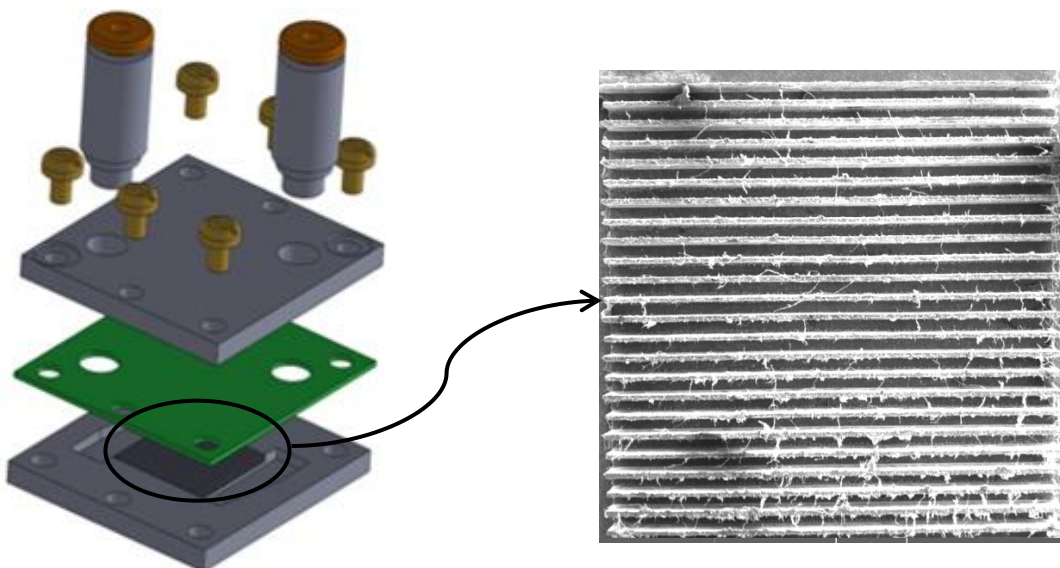


Figure 1. Microchannel heat exchanger exploded view.

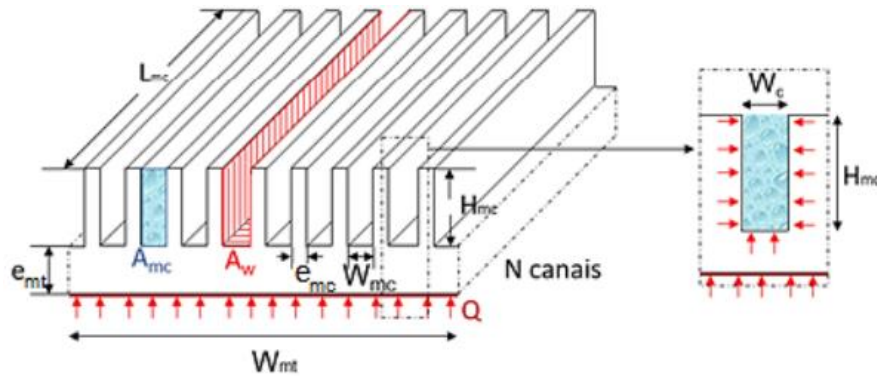


Figure 2. Geometric parameters used in the heat transfer calculation in the microchannel heat exchanger.

Tabela 1. Parâmetros geométricos do trocador de microcanais.

Description	Symbol	Value
Width of the area occupied by microchannels	$W_{mt}$	13.28 mm
Microchannels width	$W_{mc}$	400 $\mu\text{m}$
Microchannels height	$H_{mc}$	945 $\mu\text{m}$
Wall thickness between microchannels	$e_{mc}$	160 $\mu\text{m}$
Microchannels Length	$L_{mc}$	13 mm
Microchannel heat exchanger base thickness	$e_{mt}$	2.05 mm
Number of microchannels in the heat exchanger	$N_{mc}$	24
Equivalent hydraulic diameter	$D_h$	562 $\mu\text{m}$
Microchannel aspect ratio	$\alpha$	2.36
Microchannel cross sectional	$A_{mc}$	0.378 mm <sup>2</sup>
Total heat exchange area in microchannels	$A_w$	29.77 mm <sup>2</sup>

## 2.2 Convective heat transfer coefficient

Realizing energy balances on the microchannels internal surface, it can be affirmed that the convective heat transferred from the microchannel is equal to the fluid gain. In this way the convection heat transfer coefficient to the fluid is calculated by Eq. (1), where the log mean temperature difference is defined by Eq. (2).

$$h_f = \frac{Q_f}{A_w \cdot LMTD} \quad (1)$$

$$LMTD_{conv} = \frac{(T_{bi} - T_{in}) - (T_{bi} - T_{out})}{\ln\left(\frac{T_{bi} - T_{in}}{T_{bi} - T_{out}}\right)} \quad (2)$$

Where  $T_{bi}$  is the microchannel internal temperature wall that relates the upper base temperature  $T_{bs}$  according to Eq. (3) obtained from the thermal resistance concept that models the heat transferred diffusive process at the base of the microchannel heat exchanger.  $T_{in}$  and  $T_{out}$  were respectively the inlet and the outlet heat exchange temperature

$$T_{bi} = T_{bs} - \frac{Q_e \cdot A_{mt} \cdot e_{mt}}{K_{mt}} \quad (3)$$

Where  $Q_e$  is the electrical heat transfer,  $A_{mt}$  is the thermal area,  $e_{mt}$  is the microchannel heat exchanger base thickness and  $K_{mt}$  is the thermal conductivity of the micro exchanger.

All the fluids properties were calculated considering the average fluid temperature between the inlet and outlet temperatures in the test section, being considered as the reference temperature. The distilled water thermophysical properties in the energy balance calculations were determined as a function of temperature using the EES software.

### 2.3 Sieder e Tate empirical correlation

In order to analyze the experimental results of convective heat transfer, it is possible to compare them with classical empirical correlation in the literature for the convective heat transfer coefficient in laminar flow.

The convective heat transfer analysis was performed by comparing the experimental data obtained in this work with the data obtained from Sieder and Tate (1936) empirical correlation in Eq. (5), considering fully developed flow and laminar regime. Where  $\mu_{bi}$  is the fluid dynamic viscosity calculated considering the microchannel internal temperature wall  $T_{bi}$  as reference.

$$Nu = 1.86 \left[ \left( \frac{Dh}{L_{mc}} \right) \cdot Re \cdot Pr \right]^{1/3} \cdot \left( \frac{\mu}{\mu_{bi}} \right)^{0.14} \quad (5)$$

### 2.4 Shah e London empirical correlation

Additional analyses were realized using experimental results and Shah and London (1978) empirical correlation presented in Eq. (6).

$$Nu = \begin{cases} 1.953 \left( \frac{Re \cdot Pr \cdot Dh}{L} \right)^{1/3} & \left( \frac{Re \cdot Pr \cdot Dh}{L} \right) \geq 33.3 \\ 4.364 + 0.0722 \left( \frac{Re \cdot Pr \cdot Dh}{L} \right) & \left( \frac{Re \cdot Pr \cdot Dh}{L} \right) \leq 33.3 \end{cases} \quad (6)$$

### 2.5 Friction factor

With the results obtained from the pressure transmitters together with the data obtained from the differential transducer. Using Eq. (7) the fluid flowing Darcy factor through the microchannel heat exchanger was estimated.

$$f_{exp} = \frac{\Delta P_{exp} \cdot D_h}{2 \cdot L_{mc} \cdot \rho \cdot V^2} \quad (7)$$

Where  $V$  is the fluid average velocity,  $\Delta P_{exp}$  is the experimental differential pressure,  $D_h$  is the hydraulic diameter and  $L_{mc}$  microchannels length. The friction factor experimental results were compared the correlations proposed by Shah and London (1978) for fully developed laminar regime flow in rectangular channels, Eq. (8), the variable  $\alpha_c$  is the inverse of the aspect ratio ( $1/\alpha_c$ ).

$$f_{SL} Re = 96 (1 - 1,3553\alpha_c + 1,9467\alpha_c^2 - 1,7012\alpha_c^3 + 0,9564\alpha_c^4 - 0,2537\alpha_c^5) \quad (8)$$

The friction factor experimental results were also compared with the Hagen-Poiseuille distribution described in Eq. (9).

$$f = \frac{64}{Re} \quad (9)$$

## 3. RESULTS

### 3.1 Convective heat transfer coefficient and Nusselt number

The analysis of the convection heat transfer results and the calculations performed by the evaluated correlations are observed through Figures 3a – 3d, the experimental and theoretical data are presented with the convection heat transfer coefficient as a function of the mass velocity. In the Figures 4a – 4d show the Nusselt number as a function of the Reynolds number for distilled water. When analyzing the distilled water data, it was observed that the convective heat transfer coefficient results showed good agreement in comparison with the correlations chosen in the literature. The results obtained from the mean deviations were 4.55%, 4.97%, 5.86% and 6.35% for Sieder and Tate with used powers of 5 W, 15 W, 25 W and 35 W respectively, and 2.68 %, 2.77 %, 4.18 % and 4.79 % for the Shah and London correlation under the same used powers.

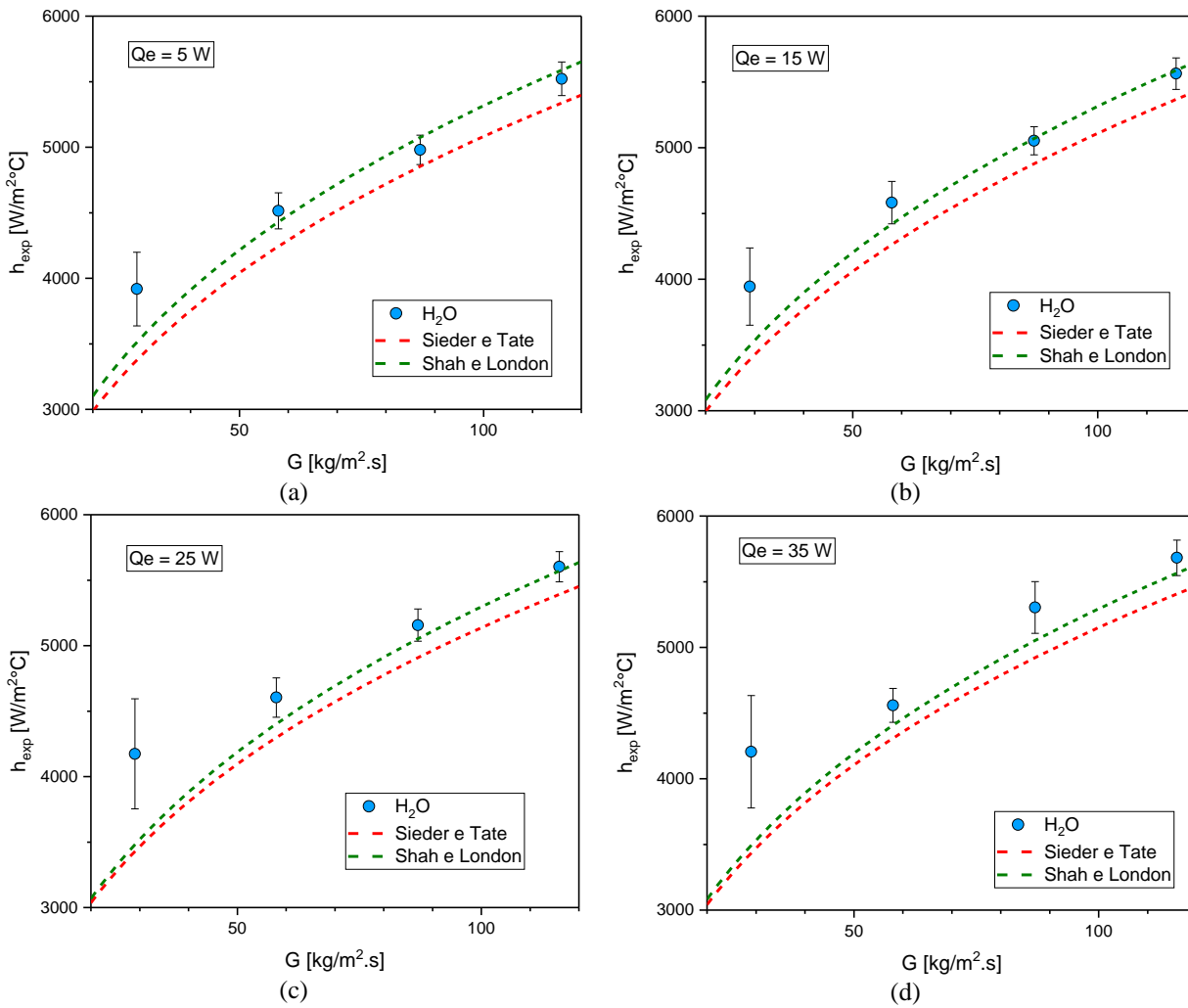


Figure 3. Convective heat transfer coefficient in function of mass velocity for distilled water: (a)  $Q_e = 5 \text{ W}$ ; (b)  $Q_e = 15 \text{ W}$ ; (c)  $Q_e = 25 \text{ W}$  and (d)  $Q_e = 35 \text{ W}$ .

Figures 4a - 4d show that for lower mass velocity values the correlations of Sieder and Tate and Shah and London were not able to represent the Nusselt number, however for higher mass velocities the correlation of Shah and London is able to adequately model the Nusselt number. The deviations obtained for the Nusselt number with the correlations in relation to the experimental data were 4.53 %, 4.64 %, 5.00 % and 6.38 % for Sieder and Tate with used powers of 5 W, 15 W, 25 W and 35 W respectively, and 2.57 %, 2.54 %, 3.31 % and 3.81 % for the Shah and London correlation under the same powers used. It is also possible to observe the effect of the supplied power, where for the highest powers the experimental results exhibit a greater deviation from the results obtained through the correlations.

Taking into account that the smallest deviations were obtained with the Shah and London correlation for the convective heat transfer coefficient analysis with powers of 5, 15, 25 and 35 W. The Figure 5 presents the comparison between the experimental data and the correlation results for pure water, it can be seen that the average deviation between the data was 5.1%, except the lowest mass velocities represented by the lowest convective heat transfer coefficients.

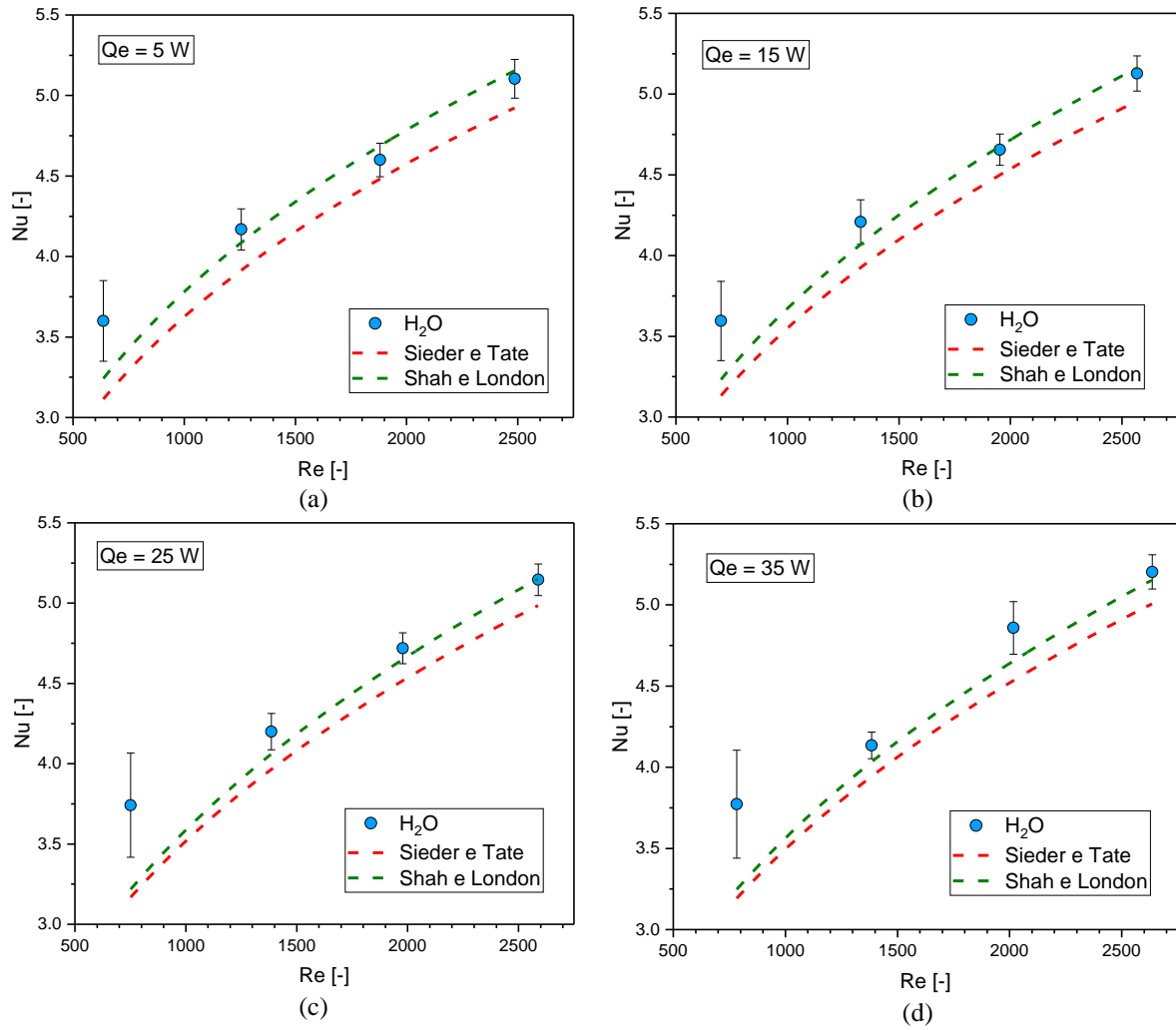


Figure 4. Nusselt number in function Reynolds number for distilled water: (a)  $Q_e = 5 \text{ W}$ ; (b)  $Q_e = 15 \text{ W}$ ; (c)  $Q_e = 25 \text{ W}$  and (d)  $Q_e = 35 \text{ W}$ .

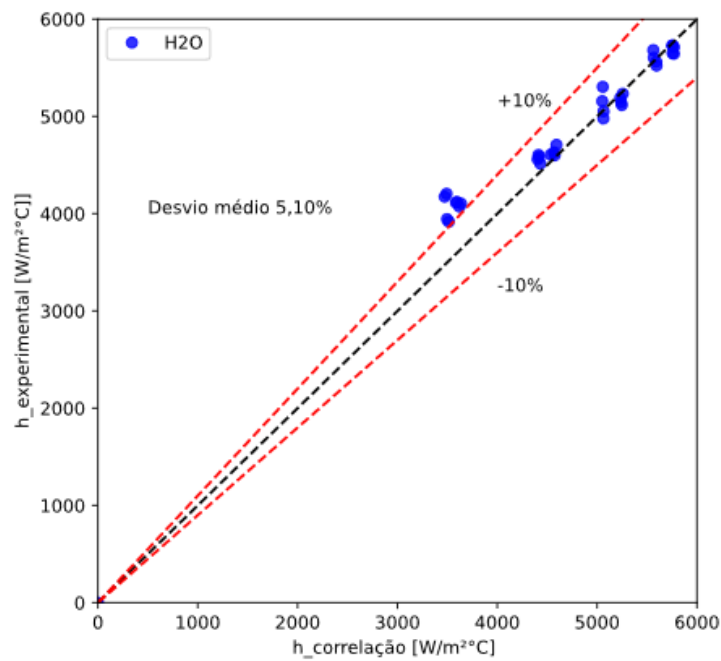


Figure 5. Experimental data with Shah and London correlation.

### 3.2 Friction Factor, pressure losses e pumping power

The Shah and London model allowed establishing that the friction factor and the Reynolds number are related through  $fRe = 64.63$ , showing a deviation of less than 2% compared to the Hagen-Poiseuille distribution. Consequently, the Figure 6 presents the behavior of the experimental friction factor when compared with the Hagen-Poiseuille distribution.

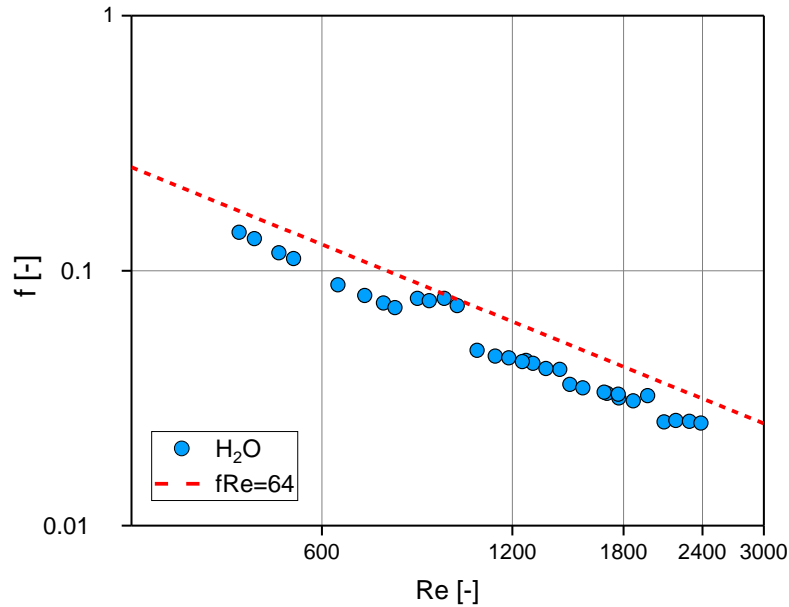


Figure 6. Experimental friction factor for water as a function of Reynolds number.

Thus, the analysis of Figure 6 shows that the friction factor has an acceptable fit with the Hagen-Poiseuille distribution. However, the experimental data showed lower values than the distribution. The comparison of the mean deviations between the experimental data and the values obtained by Eq. (8) were 6.89% for distilled water.

The experimental pressure drop in relation to the mass velocity in the Figure 7 were compared with the test conditions from the work of Peñaranda (2020) for a mixture of water and ethylene glycol (50:50) for the same heat exchanger. In this way, it is possible to establish a better hydraulic performance for water, taking into account that the pressure drop influences the thermo-hydraulic performance of heat exchangers with microchannels.

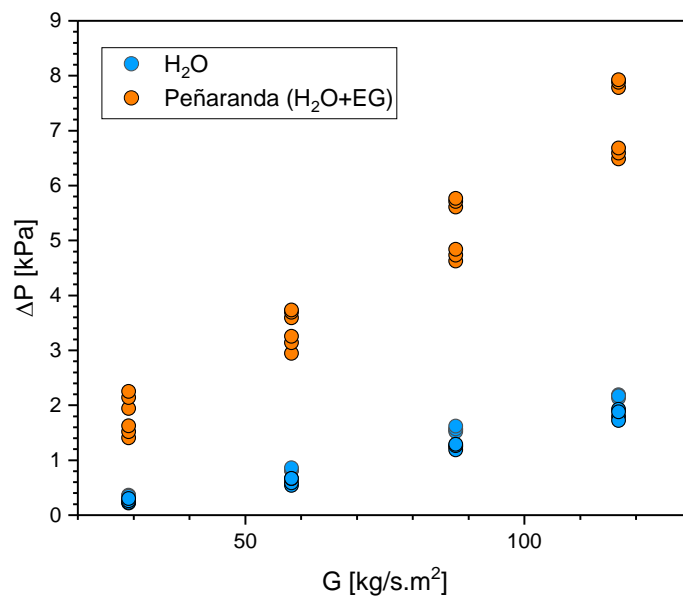


Figure 7. The experimental pressure drops in relation to the mass velocity heat for exchangers with microchannels.

Through Figure 7 it is also possible to analyze that the pressure drop presents a behavior directly proportional to the mass velocity, and the water and ethylene glycol mixture presents the highest pressure drop values and the greatest dispersion between the data found for each mass velocity value. Thus, comparing the analyzed fluid pressure drop values for the same conditions in the tests, the water and ethylene glycol mixture presents a pressure drop 309.28% greater than distilled water.

The pumping power calculation is presented Figure 8 for distilled water and the water and ethylene glycol mixture Peñaranda (2020) results.

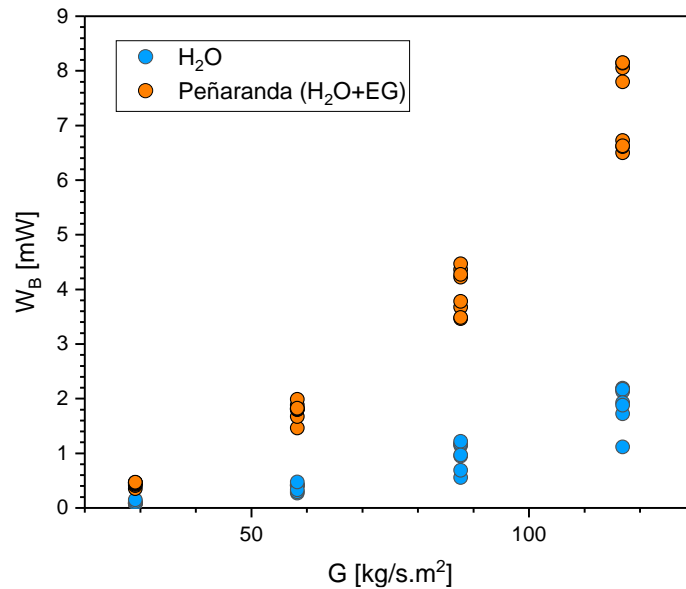


Figure 8. Pumping power.

The Figure 8 shows that the pumping power and pressure drop (Figure 7) have the same tendency, the two parameters are directly proportional in relation to the mass velocity increments. The maximum values of pumping power were respectively 2.17 mW and 8.0 mW for distilled water and the water and ethylene glycol mixture.

#### 4. CONCLUSIONS

The energy balance results applied on the experimental bench, using distilled water as working fluid, showed mean deviations smaller than 10% both correlation analyzed.

The analyzed correlations presented agreement in relation to the experimental results of energy balance for convective heat transfer coefficient with distilled water, main for high mass velocity. The values obtained from the average of the deviations were 4.55%, 4.97%, 5.86% and 6.35% for Sieder and Tate, and 2.68%, 2.77%, 4.18% and 4.79% for the Shah and London correlation, for power conditions of 5 W, 15 W, 25 W and 35 W. It can be concluded from these correlations chosen in the literature that Shah and London correlation is the most recommended in the evaluation of the thermal performance of water distilled as working fluid in heat exchangers with rectangular microchannels.

In terms of pressure loss and pumping power, the experimental Darcy friction factor were adequately represented by the literature data and water presented better performances in the pumping power when compared with the water and ethylene glycol mixture data.

#### 5. ACKNOWLEDGEMENTS

The authors gratefully acknowledge the support given to this investigation by CAPES, CNPq and FAPEMIG.

#### 6. REFERENCES

- Alfaryjat, A. A., Mohammed, H. A., Adam, N. M., Stanciu, D., & Dobrovicescu, A. (2018). Numerical investigation of heat transfer enhancement using various nanofluids in hexagonal microchannel heat sink. *Thermal Science and Engineering Progress*, 5, 252–262. <https://doi.org/10.1016/j.tsep.2017.12.003>
- Anbumeenakshi, C., & Thansekhar, M. R. (2014). Experimental Investigation of the Combined Effect of Coating and Header Combination in Microchannels. *Procedia Technology*, 14, 520–527. <https://doi.org/10.1016/j.protcy.2014.08.066>

- Esmaili, Q., Ranjbar, A. A., & Porkhial, S. (2018). Experimental analysis of heat transfer in ribbed microchannel. *International Journal of Thermal Sciences*, 130, 140–147. <https://doi.org/10.1016/j.ijthermalsci.2018.04.020>
- Fernandes, de S. (2017). *SIMULAÇÃO E EXPERIMENTOS EM MICROSSISTEMA DE RESFRIAMENTO ATIVO PARA CÉLULAS FOTOVOLTAICAS DE ALTA CONCENTRAÇÃO (HCPV)*. 185.
- Khoshvaght-Aliabadi, M., Hassani, S. M., & Mazloumi, S. H. (2017a). Enhancement of laminar forced convection cooling in wavy heat sink with rectangular ribs and Al<sub>2</sub>O<sub>3</sub>/water nanofluids. *Experimental Thermal and Fluid Science*, 89, 199–210. <https://doi.org/10.1016/j.expthermflusci.2017.08.017>
- Khoshvaght-Aliabadi, M., Hassani, S. M., & Mazloumi, S. H. (2017b). Performance enhancement of straight and wavy miniature heat sinks using pin-fin interruptions and nanofluids. *Chemical Engineering and Processing: Process Intensification*, 122, 90–108. <https://doi.org/10.1016/j.cep.2017.10.002>
- Lee, Y. J., Lee, P. S., & Chou, S. K. (2012). Enhanced thermal transport in microchannel using oblique fins. *Journal of Heat Transfer*, 134(10). <https://doi.org/10.1115/1.4006843>
- Mohammed Adham, A., Mohd-Ghazali, N., & Ahmad, R. (2013). Thermal and hydrodynamic analysis of microchannel heat sinks: A review. In *Renewable and Sustainable Energy Reviews* (Vol. 21, pp. 614–622). <https://doi.org/10.1016/j.rser.2013.01.022>
- Morini, G. L., & Brandner, J. J. (2018). The design of mini/micro heat exchangers: A world of opportunities and constraints. *International Heat Transfer Conference*, 469–486. <https://doi.org/10.1615/ihtc16.kn.000028>
- Mukesh Kumar, P. C., & Arun Kumar, C. M. (2020). Numerical study on heat transfer performance using Al<sub>2</sub>O<sub>3</sub>/water nanofluids in six circular channel heat sink for electronic chip. *Materials Today: Proceedings*, 21, 194–201. <https://doi.org/10.1016/j.matpr.2019.04.220>
- Pan, M., Wang, H., Zhong, Y., Hu, M., Zhou, X., Dong, G., & Huang, P. (2019). Experimental investigation of the heat transfer performance of microchannel heat exchangers with fan-shaped cavities. *International Journal of Heat and Mass Transfer*, 134, 1199–1208. <https://doi.org/10.1016/j.ijheatmasstransfer.2019.01.140>
- Pandey, J., Husain, A., Zahid Ansari, M., & Al-Azri, N. (2022). Comparison of the parallel microchannel and Pin-Fin heat Sinks: An experimental study. *Materials Today: Proceedings*. <https://doi.org/10.1016/j.matpr.2022.02.503>
- PEÑARANDA, L. E. (2020). *Estudo experimental dos métodos ativo e passivo para arrefecimento de painéis fotovoltaicos de alta concentração*. Universidade Federal de Uberlândia.
- Peng, Y., Li, Z., Li, S., Cao, B., Wu, X., & Zhao, X. (2021). The experimental study of the heat transfer performance of a zigzag-serpentine microchannel heat sink. *International Journal of Thermal Sciences*, 163. <https://doi.org/10.1016/j.ijthermalsci.2021.106831>
- Rincón, E. D. (2022). *Estudo experimental do desempenho térmico de trocadores de calor tipo multi microcanais operando com nanofluidos de grafeno*. Universidade Federal de Uberlândia. <https://doi.org/10.14393/ufu.di.2023.7004>
- Shah, R. K., & London, A. L. (1978). Laminar Flow Forced Convection in Ducts. *Supplement 1 To Advances in Heat Transfer*. <http://www.sciencedirect.com/science/article/pii/B978012020051150022X>
- Sharma, C. S., Tiwari, M. K., Michel, B., & Poulikakos, D. (2013). Thermofluidics and energetics of a manifold microchannel heat sink for electronics with recovered hot water as working fluid. *International Journal of Heat and Mass Transfer*, 58(1–2), 135–151. <https://doi.org/10.1016/j.ijheatmasstransfer.2012.11.012>
- SIEDER, E. N. ;, & TATE, G. E. (1936). Heat Transfer and Pressure Drop of Liquids in Tubes. *Industrial & Engineering Chemistry*, 28, 1429–1435.
- Tuckerman, D. B., & Pease, R. F. W. (1981). High-Performance Heat Sinking for VLSI. *IEEE Electron Device Letters*, EDL-2(5), 126–129. <https://doi.org/10.1109/EDL.1981.25367>
- Xia, G. D., Jiang, J., Wang, J., Zhai, Y. L., & Ma, D. D. (2015). Effects of different geometric structures on fluid flow and heat transfer performance in microchannel heat sinks. *International Journal of Heat and Mass Transfer*, 80, 439–447. <https://doi.org/10.1016/j.ijheatmasstransfer.2014.08.095>
- Xia, G., Ma, D., Zhai, Y., Li, Y., Liu, R., & Du, M. (2015). Experimental and numerical study of fluid flow and heat transfer characteristics in microchannel heat sink with complex structure. *Energy Conversion and Management*, 105, 848–857. <https://doi.org/10.1016/j.enconman.2015.08.042>
- Yang, L., & Du, K. (2020). Numerical simulation of nanofluid flow and heat transfer in a microchannel: The effect of changing the injection layout arrangement. *International Journal of Mechanical Sciences*, 172. <https://doi.org/10.1016/j.ijmecsci.2019.105415>
- Zhong, T. M., Chen, Y., Zheng, W. X., Hua, N., Luo, X. L., Yang, Q. C., Mo, S. P., & Jia, L. S. (2014). Experimental investigation on microchannel condensers with and without liquid-vapor separation headers. *Applied Thermal Engineering*, 73(2), 1510–1518. <https://doi.org/10.1016/j.applthermaleng.2014.08.047>

## 7. RESPONSIBILITY NOTICE

The authors are the only responsible for the printed material included in this paper.